Online Appendix for "Balancing Cost and Service: Charging Rate Optimization for EV Battery Swapping"

Bo Feng, Hailong Sun

Appendix A: Proofs

Proof of Theorem 1. To prove the theorem, we first prove a few supporting lemmas.

The first lemma says that it is without loss of optimality for the BSS to charge the SOC of batteries no more than α_0.

LEMMA 1. *Let $\boldsymbol{s}_t$ and $\boldsymbol{s}'_t$ be two state variables, with $s_{j,t} = \alpha_0$ and $\alpha_0 < s'_{j,t} \leq 1$ for some j, and $s_{i,t} = s'_{i,t}$ for any $i \neq j, i \in [K]$. Then $V_t^*(\boldsymbol{s}_t, N_{f,t}) = V_t^*(\boldsymbol{s}'_t, N_{f,t})$.*

Proof of Lemma 1. Consider $V_t^*(\boldsymbol{s}_t, N_{f,t})$ and $V_t^*(\boldsymbol{s}'_t, N_{f,t})$ for some fixed $N_{f,t}$, and assume that there exists a feasible decision $\boldsymbol{z}'_t$ satisfying the service level constraint and capacity constraint in $V_t^*(\boldsymbol{s}'_t, N_{f,t})$. Note that it is easy to verify the feasibility of the service level constraint given the demand distribution, since the left-hand side expected value is monotone increasing in $\boldsymbol{z}_t$ for given $N_{f,t}$. In addition, it is easy to see that any optimal solution to $V_t^*(\boldsymbol{s}'_t, N_{f,t})$ is feasible to $V_t^*(\boldsymbol{s}_t, N_{f,t})$ as well. If the optimal solution $z'^*_{j,t} = 1$, then we have $V_t^*(\boldsymbol{s}_t, N_{f,t}) = V_t^*(\boldsymbol{s}'_t, N_{f,t})$ by setting $\boldsymbol{z}_t^* = \boldsymbol{z}'^*_t$ because $\boldsymbol{s}_{t+1} = \boldsymbol{s}'_{t+1}$. Otherwise, if $z'^*_{j,t} = 0$, then there must exists some time period $t' > t$ such that $z'^*_{j,t'} = 1$, and this solution must be feasible to $V_t^*(\boldsymbol{s}_t, N_{f,t})$ as well. By the Bellman equation we have $V_t^*(\boldsymbol{s}_t, N_{f,t}) = V_t^*(\boldsymbol{s}'_t, N_{f,t})$. $\square$

The next lemma establish the nonincreasing property of the optimal cost-to-go.

LEMMA 2. *$V_t^*(\cdot, N_{f,t})$ is monotone nonincreasing, that is, $V_t^*(\boldsymbol{s}_t, N_{f,t}) \geq V_t^*(\boldsymbol{s}'_t, N_{f,t})$ for any $\boldsymbol{s}_t \leq \boldsymbol{s}'_t \leq \alpha_0$ (elementwise).*

Proof of Lemma 2. Without loss of generality, let $S_t := \{i : s_{i,t} = \alpha_0, i \in [K]\}$ and $S'_t := \{i : s'_{i,t} = \alpha_0, i \in [K]\}$. Then we have $S_t \subseteq S'_t$ because $\boldsymbol{s}_t \leq \boldsymbol{s}'_t \leq \alpha_0$. We prove the monotonicity by induction. First, by definition $V_{T+1}^*(\boldsymbol{s}_{T+1}, N_{f,T+1})$ is clearly nonincreasing s_{T+1}. Assume that $V_{t+1}^*(\boldsymbol{s}_{t+1}, N_{f,t+1})$ is nonincreasing for fixed $N_{f,t+1}$. Consider the following reformulation of the Bellman equation:

$$\begin{aligned} V_t^*(\boldsymbol{s}_t, N_{f,t}) = \min_{\boldsymbol{s}_{t+1}, \boldsymbol{z}_t} & \sum_{i\in[K]} \left[p_t(s_{i,t+1} - s_{i,t}(1-z_{i,t}) - s^{(0)} z_{i,t}) + h(s_{i,t+1} - s_{i,t}(1-z_{i,t}) - s^{(0)} z_{i,t})\right] \\ & + \mathbb{E}\left[V_{t+1}^*\left(\boldsymbol{s}_{t+1}, N_{f,t} + \sum_{i\in[K]} z_{i,t} - \tilde{d}_t\right)\right] \end{aligned} \tag{21}$$

where $s_{i,t+1} \geq s_{i,t}(1-z_{i,t}) + s^{(0)} z_{i,t}$ for $i \in [K]$. Let $(\boldsymbol{s}_{t+1}^*(\boldsymbol{s}_t), \boldsymbol{z}_t^*(\boldsymbol{s}_t))$ and $(\boldsymbol{s}'^*_{t+1}(\boldsymbol{s}'_t), \boldsymbol{z}'^*_t(\boldsymbol{s}'_t))$ be the optimal solution to $V_t^*(\boldsymbol{s}_t, N_{f,t})$ and $V_t^*(\boldsymbol{s}'_t, N_{f,t})$ correspondingly for fixed $N_{f,t}$. By Lemma 1 it is without loss of optimality to consider optimal solutions $s_{t+1}^* \leq \alpha_0$ and $s'^*_{t+1} \leq \alpha_0$. Note that $z_{i,t}^* = 0$ for any $i \notin S_t$ due to the feasibility constraint $\alpha_0 z_{i,t} \leq s_{i,t}$. By contrast, $z_{i,t}^* \in \{0,1\}$ for $i \in S_t$.

Now we construct a feasible solution to $V_t^*(\boldsymbol{s}'_t, N_{f,t})$ in (21). Let $z'_{i,t} = z^*_{i,t} = 0$ and $s'_{i,t+1} = s^*_{i,t+1} \vee s'_{i,t}$ for $i \in [K] \setminus S_t$, where $a \vee b := \max\{a, b\}$, and let $z'_{i,t} = z^*_{i,t}$ and $s'_{i,t+1} = s^*_{i,t+1}$ for $i \in S_t$. We claim that $(\boldsymbol{s}'_{t+1}, \boldsymbol{z}'_t) := (s'_{i,t+1}, z'_{i,t})_{i\in[K]}$ is feasible to (21), that is, it satisfies $s'_{i,t+1} \geq s'_{i,t}(1-z'_{i,t}) + s^{(0)} z'_{i,t}$ for $i \in [K]$. To see this, first, note that $(s'_{i,t+1}, z'_{i,t}) = (s^*_{i,t+1} \vee s'_{i,t}, 0)$ is feasible for $i \in [K] \setminus S_t$, because $s^*_{i,t+1} \vee s'_{i,t} \geq s'_{i,t} = s'_{i,t}(1 - z'_{i,t}) + s^{(0)} z'_{i,t}$ if $z'_{i,t} = z^*_{i,t} = 0$, which is feasible because $S_t \subseteq S'_t$; Second, for all $i \in S_t$, if $z'_{i,t} = z^*_{i,t} = 0$, then $s'_{i,t+1} = s^*_{i,t+1} \geq s_{i,t} = s'_{i,t} = \alpha_0$ by Lemma 1, which is feasible. On the other hand, if $z'_{i,t} = z^*_{i,t} = 1$, then $s'_{i,t+1} = s^*_{i,t+1} \geq s^{(0)}$, showing that it is still feasible.

Next, we have the following inequality

$$s^*_{i,t+1} - s'_{i,t}(1 - z^*_{i,t}) \leq s^*_{i,t+1} - s_{i,t}(1 - z^*_{i,t}) \quad \forall i \in S_t, \tag{22}$$

which follows from the fact that $s'_{i,t} \geq s_{i,t}$ and $1 - z^*_{i,t} \geq 0$. In addition, for all $i \in [K] \setminus S_t$ we have either

$$s^*_{i,t+1} \vee s'_{i,t} - s'_{i,t} = s^*_{i,t+1} - s'_{i,t} \leq s^*_{i,t+1} - s_{i,t}$$

or

$$s^*_{i,t+1} \vee s'_{i,t} - s'_{i,t} = s'_{i,t} - s'_{i,t} = 0 \leq s^*_{i,t+1} - s_{i,t}.$$

Therefore, the following inequality holds

$$(s^*_{i,t+1} \vee s'_{i,t}) - s'_{i,t} \leq s^*_{i,t+1} - s_{i,t} \quad \forall i \in [K] \setminus S_t. \tag{23}$$

Finally, we have

$$\begin{aligned}
V^*_t(\boldsymbol{s}'_t, N_{f,t}) \leq & \sum_{i \in S_t} \left[p_t(s^*_{i,t+1} - s'_{i,t}(1 - z^*_{i,t}) - s^{(0)} z^*_{i,t}) + h(s^*_{i,t+1} - s'_{i,t}(1 - z^*_{i,t}) - s^{(0)} z^*_{i,t}) \right] + \\
& \sum_{i \notin S_t} \left[p_t((s^*_{i,t+1} \vee s'_{i,t}) - s'_{i,t}) + h((s^*_{i,t+1} \vee s'_{i,t}) - s'_{i,t}) \right] \\
& + \mathbb{E}\left[V^*_{t+1}(\boldsymbol{s}'_{t+1}, N_{f,t} + \sum_{i \in [K]} z^*_{i,t} - \tilde{d}_t) \right] \\
\leq & \sum_{i \in S_t} \left[p_t(s^*_{i,t+1} - s_{i,t}(1 - z^*_{i,t}) - s^{(0)} z^*_{i,t}) + h(s^*_{i,t+1} - s_{i,t}(1 - z^*_{i,t}) - s^{(0)} z^*_{i,t}) \right] + \\
& \sum_{i \notin S_t} \left[p_t(s^*_{i,t+1} - s_{i,t}) + h(s^*_{i,t+1} - s_{i,t}) \right] \\
& + \mathbb{E}\left[V^*_{t+1}(\boldsymbol{s}^*_{t+1}, N_{f,t} + \sum_{i \in [K]} z^*_{i,t} - \tilde{d}_t) \right] \\
= & \sum_{i \in [K]} \left[p_t(s^*_{i,t+1} - s_{i,t}(1 - z^*_{i,t}) - s^{(0)} z^*_{i,t}) + h((s^*_{i,t+1}) - s_{i,t}(1 - z^*_{i,t}) - s^{(0)} z^*_{i,t}) \right] \\
& + \mathbb{E}\left[V^*_{t+1}(\boldsymbol{s}^*_{t+1}, N_{f,t} + \sum_{i \in [K]} z^*_{i,t} - \tilde{d}_t) \right] \\
= & V^*_t(\boldsymbol{s}_t, N_{f,t}),
\end{aligned}$$

where the first inequality follows from the feasibility of $(\boldsymbol{s}'_{t+1}, \boldsymbol{z}'_t)$. To see the second inequality, note that $V^*_{t+1}(\cdot, N_{f,t+1})$ is nonincreasing by assumption. Since $\boldsymbol{s}'_{t+1} \geq \boldsymbol{s}^*_{t+1}$, we have

$$V^*_{t+1}\left(\boldsymbol{s}'_{t+1}, N_{f,t} + \sum_{i \in [K]} z^*_{i,t} - \tilde{d}_t \right) \leq V^*_{t+1}\left(\boldsymbol{s}^*_{t+1}, N_{f,t} + \sum_{i \in [K]} z^*_{i,t} - \tilde{d}_t \right)$$

which implies that

$$\mathbb{E}\left[V_{t+1}^*\left(\boldsymbol{s}'_{t+1}, N_{f,t}+\sum_{i\in[K]} z_{i,t}^* - \tilde{d}_t\right)\right] \le \mathbb{E}\left[V_{t+1}^*\left(\boldsymbol{s}^*_{t+1}, N_{f,t}+\sum_{i\in[K]} z_{i,t}^* - \tilde{d}_t\right)\right]$$

Combining with inequalities (22) and (23) we obtain the second inequality. The proof is complete. □

Given the above two lemmas, we then characterize the optimal loading/unloading decision $\boldsymbol{z}_t^*$. To analyze the optimal $z_{i,t}^*$ for $i \in S_t$, it suffices to consider the case $|S_t| \le N - K - N_{f,t}$. Consider two feasible decisions $(\boldsymbol{z}_t, \boldsymbol{x}_t)$ and $(\boldsymbol{z}'_t, \boldsymbol{x}_t)$ to the minimization problem of $V_t^*(\boldsymbol{s}_t, N_{f,t})$ with some $i \in S_t$, and the only difference between these decisions is $z_{i,t} = 1$ and $z'_{i,t} = 0$. In addition, for all $t' > t$ we keep the decisions for both feasible solutions the same. Following similar reasoning to the above, there must exists some $t' > t$ such that $z'_{i,t'} = 1$. In particular, the costs incurred for these two decisions before $t'+1$ and the available batteries for swapping $N_{f,t'+1}$ are the same. The only difference is the optimal cost-to-go of period $t'+1$. Let $V^*(\boldsymbol{s}_{t'+1}, N_{f,t'+1})$ be the cost-to-go corresponding to decision $(\boldsymbol{z}_t, \boldsymbol{x}_t)$, and let $V^*(\boldsymbol{s}'_{t'+1}, N_{f,t'+1})$ be the cost-to-go corresponding to decision $(\boldsymbol{z}'_t, \boldsymbol{x}_t)$. By Lemma 2 we have $V^*(\boldsymbol{s}_{t'+1}, N_{f,t'+1}) \le V^*(\boldsymbol{s}'_{t'+1}, N_{f,t'+1})$ since $s_{t'+1} \ge s'_{t'+1}$. Thus, it is optimal to set $z_{i,t}^* = 1$ for any $i \in S_t$, and part (i) of the proposition is proved.

To see part (ii), note that given the optimal decision $\boldsymbol{z}_t^*$ we can reformulate the Bellman equation as follows:

$$\begin{aligned} V_t^*(\boldsymbol{s}_t, N_{f,t}) = \min_{\boldsymbol{s}_t \le \boldsymbol{s}_{t+1} \le \alpha_0} p_t \cdot \sum_{i\in S_t}(s_{i,t+1} - s^{(0)}) + p_t \cdot \sum_{i\notin S_t}(s_{i,t+1} - s_{i,t}) + \sum_{i\in S_t} h(s_{i,t+1} - s^{(0)}) \\ + \sum_{i\notin S_t} h(s_{i,t+1} - s_{i,t}) + \mathbb{E}(V_{t+1}^*(\boldsymbol{s}_{t+1}, N_{f,t+1})) \end{aligned}$$

We prove the convexity $V_t^*(\cdot, N_{f,t})$ by induction. First, note that $V_{T+1}^*(\cdot, N_{f,T+1}) = C \cdot \mathbb{E}\left[(-N_{f,T+1})^+\right]$, which is clearly convex in $\boldsymbol{s}_{T+1}$. Now assume that $V_{t+1}^*(\cdot, N_{f,t+1})$ is convex. Taking expectation preserves the convexity, thus $\mathbb{E}(V_{t+1}^*(\cdot, N_{f,t+1}))$ is convex. In addition, note that the objective function within the above minimization problem is jointly convex in $(\boldsymbol{s}_{t+1}, \boldsymbol{s}_t)$. Therefore, $V_t^*(\boldsymbol{s}_t, N_{f,t})$ is convex in $\boldsymbol{s}_t$, and there exists some thresholds $\boldsymbol{s}_{t+1}^*$ such that it is optimal to increase $s_{i,t}$ to $s_{i,t+1}^*$ if $s_{i,t} < s_{i,t+1}^*$, and keep $s_{i,t}$ unchanged if $s_{i,t} \ge s_{i,t+1}^*$. □

Proof of Corollary 1. Since $y_{i,t,l}$ is binary, the convexity of $V_t^*(\cdot, N_{f,t})$ no longer holds. However, given the optimal decision $\boldsymbol{z}_t^*$ we can reformulate the Bellman equation as follows:

$$\begin{aligned} V_t^*(\boldsymbol{s}_t, N_{f,t}) = \min_{\boldsymbol{s}_{t+1} \le \alpha_0} p_t \cdot \sum_{i\in S_t}(s_{i,t+1} - s^{(0)}) + p_t \cdot \sum_{i\notin S_t}(s_{i,t+1} - s_{i,t}) + \sum_{i\in S_t} h(s_{i,t+1} - s^{(0)}) \\ + \sum_{i\notin S_t} h(s_{i,t+1} - s_{i,t}) + \mathbb{E}(V_{t+1}^*(\boldsymbol{s}_{t+1}, N_{f,t+1})), \end{aligned}$$

where the optimal decision $s_{i,t+1}^*$ must take one of the $L+1$ candidate values: $s_{i,t}, s_{i,t}+x_1, \ldots, s_{i,t}+x_L$. The result then follows directly. □

Proof of Proposition 1. Let π^* denote the optimal dynamic policy of the stochastic DP under initial system state $(\boldsymbol{s}_1, N_{f,1})$, and let $(\boldsymbol{x}_t^*(\boldsymbol{s}_t^*, N_{f,t}^*), \boldsymbol{z}_t^*(\boldsymbol{s}_t^*, N_{f,t}^*))_{t\in[T]}$ be the corresponding optimal decision under π^* with respect to sample path $(\bar{D}_t)_{t\in[T]}$. Note that π^* specifies the mapping from states to charging/loading decisions under any demand sample path. Since $\tilde{d}_t$ is random, all the system state and decision variables are also random. Let $\bar{\pi}^* := \mathbb{E}[\pi^*]$ denote the deterministic policy averaged over all demand sample paths. We shall omit the dependence of policy on state variables when the context is clear.

We first show that $\bar{\pi}^*$ is feasible for the linear relaxation of static optimization model (12) under sample path $(\bar{D}_t)_{t\in[T]}$. To see this, note that we can construct the corresponding McCormick envelope constraints for π^* in the form of (11). Now because the battery inventory dynamics and the McCormick envelopes (battery charging constraints) are all linear, taking expectations over these constraints yields

$$\mathbb{E}\left[N^*_{f,t+1}\right] = \mathbb{E}\left[N^*_{f,t}\right] + \sum_{i\in[K]} \mathbb{E}\left[z^*_{i,t}\right] - \bar{D}_t, \quad \sum_{i\in[K]} \mathbb{E}\left[z^*_{i,t}\right] \le N - K - \mathbb{E}\left[\left(N^*_{f,t}\right)^+\right] \le N - K - \left(\mathbb{E}\left[N^*_{f,t}\right]\right)^+ \quad \forall t\in[T]$$

and

$$\begin{cases} \mathbb{E}\left[s^*_{i,t+1}\right] = \mathbb{E}\left[s^*_{i,t}\right] - \mathbb{E}\left[q^*_{i,t}\right] + \eta_i \mathbb{E}\left[x^*_{i,t}\right] + s^{(0)}\mathbb{E}\left[z^*_{i,t}\right] \\ 0 \le \mathbb{E}\left[q^*_{i,t}\right] \le \mathbb{E}\left[z^*_{i,t}\right], \; \mathbb{E}\left[z^*_{i,t}\right] + \mathbb{E}\left[s^*_{i,t}\right] - 1 \le \mathbb{E}\left[q^*_{i,t}\right] \le \mathbb{E}\left[s^*_{i,t}\right], \quad \forall t\in[T] \end{cases}$$

which shows that $\bar{\pi}^*$ is feasible for the constraints regarding battery inventory dynamics and charging process.

Next, we examine the service level constraint. Since π^* is optimal for the DP formulation, we have

$$\min\left\{\mathbb{E}\left(N^*_{f,t} + \sum_{i\in[K]} z^*_{i,t}\right), \mathbb{E}\left[\tilde{d}_t\right]\right\} \ge \mathbb{E}\left[\min\left\{\left(N^*_{f,t} + \sum_{i\in[K]} z^*_{i,t}\right), \tilde{d}_t\right\}\right] \ge \gamma_t \mathbb{E}\left[\tilde{d}_t\right] \quad \forall t\in[T],$$

which implies that

$$\mathbb{E}\left[N^*_{f,t}\right] + \sum_{i\in[K]} \mathbb{E}\left[z^*_{i,t}\right] \ge \gamma_t \bar{D}_t \quad \forall t\in[T].$$

Thus, $\bar{\pi}^*$ is a feasible policy for the linear relaxation of the static optimization model.

Therefore, we have

$$\begin{aligned} Z^*_r(\boldsymbol{s}_1, N_{f,1}) &\le \sum_{t\in[T]}\sum_{i\in[K]} p_t \cdot \mathbb{E}\left[x^*_{i,t}\right] + h(\mathbb{E}\left[x^*_{i,t}\right]) + C\cdot(-\mathbb{E}\left[N^*_{f,T+1}\right])^+ \\ &= \sum_{t\in[T]}\sum_{i\in[K]} p_t \cdot \mathbb{E}\left[x^*_{i,t}\right] + h(\mathbb{E}\left[x^*_{i,t}\right]) + C\cdot\left(\bar{D}_t - \mathbb{E}\left[N^*_{f,T}\right] - \sum_{i\in[K]} \mathbb{E}\left[z^*_{i,T}\right]\right)^+ \\ &\le \sum_{t\in[T]}\sum_{i\in[K]} p_t \cdot \mathbb{E}\left[x^*_{i,t}\right] + \mathbb{E}\left[h(x^*_{i,t})\right] + C\cdot\mathbb{E}\left[\left(\tilde{d}_t - N^*_{f,T} - \sum_{i\in[K]} z^*_{i,T}\right)^+\right] \\ &= V^*_1(\boldsymbol{s}_1, N_{f,1}), \end{aligned}$$

where the first inequality holds since $\bar{\pi}^*$ is feasible for the static optimization model, and the second inequality follows from Jensen's inequality. □

Proof of Proposition 2. Let

$$\mathcal{F}_t := \left\{\Pi_t \in \mathcal{P}_0(\mathcal{D}\times\mathcal{D}) \mid (\tilde{d}_t, \hat{d}_t) \sim \Pi_t, \tilde{d}_t \sim \mathbb{P}_t, \hat{d}_t \sim \hat{\mathbb{P}}_t\right\},$$

which is the set of joint distributions Π with marginals $\mathbb{P}_t$ and $\hat{\mathbb{P}}_t$. Then we have

$$\begin{aligned} & \mathbb{E}_{\mathbb{P}_t}\left[\gamma_t \cdot \tilde{d}_t\right] - w_t \le \theta_t \cdot \Delta(\mathbb{P}, \hat{\mathbb{P}}) && \forall \mathbb{P}_t \in \mathcal{P}_t \\ \iff\; & \mathbb{E}_{\mathbb{P}_t}\left[\gamma_t \cdot \tilde{d}_t\right] - w_t \le \theta \cdot \inf_{\Pi_t\in\mathcal{F}_t}\left\{\mathbb{E}_{\Pi_t}\left[\|\tilde{d}_t - \hat{d}_t\|_1\right]\right\} && \forall \mathbb{P}_t \in \mathcal{P}_t \\ \iff\; & \mathbb{E}_{\mathbb{P}_t}\left[\gamma_t \cdot \tilde{d}_t\right] - w_t \le \theta \cdot \mathbb{E}_{\Pi_t}\left[\|\tilde{d}_t - \hat{d}_t\|_1\right] && \forall \mathbb{P}_t \in \mathcal{P}, \forall \Pi_t \in \mathcal{F}_t \\ \iff\; & \mathbb{E}_{\Pi_t}\left[\gamma_t \cdot \tilde{d}_t - w_t - \theta \cdot \|\tilde{d}_t - \hat{d}_t\|_1\right] \le 0 && \forall \Pi_t \in \mathcal{F}_t \end{aligned}$$

$$
\begin{aligned}
&\overset{(1)}{\iff} \quad \frac{1}{S}\sum_{s\in[S]} \mathbb{E}_{\mathbb{P}_{t,s}}\left(\gamma_t \cdot \tilde{d}_t - w_t - \theta \cdot \|\tilde{d}_t - \hat{d}_{t,s}\|_1\right) \le 0 && \forall \mathbb{P}_{t,s} \in \mathcal{P}_0(\mathcal{D}), s\in[S]\\
&\iff \quad \frac{1}{S}\sup_{\mathbb{P}_s\in\mathcal{P}_0(\mathcal{D})}\sum_{s\in[S]} \mathbb{E}_{\mathbb{P}_{t,s}}\left[\gamma_t \cdot \tilde{d}_t - w_t - \theta \cdot \|\tilde{d}_t - \hat{d}_{t,s}\|_1\right] \le 0\\
&\overset{(2)}{\iff} \quad \frac{1}{S}\sum_{s\in[S]}\sup_{\mathbb{P}_s\in\mathcal{P}_0(\mathcal{D})} \mathbb{E}_{\mathbb{P}_{t,s}}\left[\gamma_t \cdot \tilde{d}_t - w_t - \theta \cdot \|\tilde{d}_t - \hat{d}_{t,s}\|_1\right] \le 0\\
&\overset{(3)}{\iff} \quad \frac{1}{S}\sum_{s\in[S]}\sup_{d\in\mathcal{D}}\left[\gamma_t \cdot d_t - \theta\|d_t - \hat{d}_{t,s}\|_1\right] - w_t \le 0.
\end{aligned}
$$

In the above inequalities, (1) follows from the law of total probability, where we construct $\Pi_t = \mathbb{P}_{t,s} \bigotimes \hat{\mathbb{P}}_t$, *i.e.*, the joint distribution Π_t is constructed from the marginal distribution $\hat{\mathbb{P}}_t$ of $\hat{d}_t$ and the conditional distribution $\mathbb{P}_{t,s}$ of $\tilde{d}_t$ given $\hat{d}_t = \hat{d}_{t,s}$. (2) holds since there is no coupling constraint on the decision variables $\mathbb{P}_{t,s}$, so we can switch the order of supremum and summation. (3) follows from the fact that the optimal distribution is a one-point distribution, since there is only support constraint on the distributions $\mathbb{P}_{t,s}$.

Next, let

$$
\kappa^*_{t,s} = \sup_{d_t\in\mathcal{D}_t}\left[\gamma_t d_t - \theta\|d_t - \hat{d}_{t,s}\|_1\right] = \sup_{d_t\in\mathcal{D}_t}\left[\gamma_t d_t - \theta\left|d_t - \hat{d}_{t,s}\right|\right] \quad \forall t\in[T], s\in[S_1]
$$

Observe that we are minimizing the following piece-wise linear function over bounded intervals

$$
\gamma_t d_t - \theta\left|d_t - \hat{d}_{t,s}\right| = \begin{cases} (\gamma_t - \theta)d_t + \theta\hat{d}_{t,s} & \text{if} \quad \hat{d}_{t,s} \le d_t \le \bar{d}\\ (\gamma_t + \theta)d_t - \theta\hat{d}_{t,s} & \text{if} \quad 0 \le d_t < \hat{d}_{t,s}.\end{cases}
$$

Note that $\gamma_t \ge 0$ for all $t\in[T]$ and $\theta \ge 0$. The optimal solution to this piecewise linear optimization problem lies on the boundaries. Then it can be easily checked that κ^* can be solved to closed-form given by

$$
\kappa^*_{t,s} = \max\left\{\gamma_t\bar{d} + (\hat{d}_{t,s} - \bar{d})\theta,\ \gamma_t\hat{d}_{t,s}\right\}.
$$

Finally, we have

$$
\begin{aligned}
& \frac{1}{S}\sum_{s\in[S]}\sup_{d_t\in\mathcal{D}}\left[\gamma_t d_t - \theta\|d_t - d_{t,s}\|_1\right] - w_t \le 0 && \forall t\in[T]\\
\iff \quad & \frac{1}{S}\sum_{s\in[S]}\kappa^*_{t,s} - w_t \le 0 && \forall t\in[T]\\
\iff \quad & \frac{1}{S}\sum_{s\in[S]} v_{t,s} - w_t \le 0,\ \gamma_t\bar{d} + (\hat{d}_{t,s} - \bar{d})\theta \le v_{t,s},\ \gamma_t\hat{d}_{t,s} \le v_{t,s} && \forall t\in[T], s\in[S].
\end{aligned}
$$

□

Proof of Proposition 3. Suppose we are given some initial system state $(\boldsymbol{s}_1, N_{f,1})$, and solve the static optimization model (12) under $\hat{\boldsymbol{D}} = \bar{\boldsymbol{D}}$ to obtain optimal solutions $(\boldsymbol{x}^*_t, \boldsymbol{s}^*_{t+1}, \boldsymbol{z}^*_t, \boldsymbol{q}^*_t, N^*_{f,t})_{t\in[T]}$, and the corresponding optimal objective value $Z^*(\boldsymbol{s}_1, N_{f,1}; \bar{\boldsymbol{D}})$. Now we use these values to construct a feasible solution to the budget-driven model (20).

We set the cost budget as $\Gamma = Z^*(\boldsymbol{s}_1, N_{f,1}; \bar{\boldsymbol{D}})$, and let $w_t = \bar{D}_t$ and $\theta_t = \gamma_t = 1$ for any t. In addition, we let $v_{t,s} = \gamma_t\hat{d}_{t,s} = \hat{d}_{t,s}$ for $t\in[T], s\in[S]$. In the following, we show that $(\theta_t, w_t, \boldsymbol{x}^*_t, \boldsymbol{s}^*_{t+1}, \boldsymbol{z}^*_t, \boldsymbol{q}^*_t, \boldsymbol{v}_t)_{t\in[T]}$ is a feasible solution to the budget-driven model (20). First, note that the charging/loading decisions $(\boldsymbol{x}^*_t, \boldsymbol{s}^*_{t+1}, \boldsymbol{z}^*_t, \boldsymbol{q}^*_t)$ clearly satisfy the battery charging process constraints (2) and (11), as these constraints are shared in both models. Second, note that $\gamma_t \bar{d} + (\hat{d}_{t,s} - \bar{d})\theta_t = \hat{d}_{t,s} = v_{t,s}$ and

$$\frac{1}{S}\sum_{s\in[S]} v_{t,s} = \bar{D}_t = w_t \quad \forall t \in [T]$$

Thus, $(\theta_t, w_t, \boldsymbol{v}_t)_{t\in[T]}$ satisfy the service level constraint (16). Third, since $\boldsymbol{z}_t^*$ satisfies the inventory dynamics equation $N_{f,t+1} = N_{f,t} + \sum_{i\in[K]} z_{i,t} - \bar{D}_t$ and the capacity constraint (3), they are also feasible for inventory constraints (18). In addition, because $\gamma_t = 1$, the service level constraint becomes

$$N_{f,t} + \sum_{i\in[K]} z_{i,t} \geq \bar{D}_t,$$

showing that (19) is feasible. Finally, the cost budget constraint is also feasible, *i.e.*,

$$\sum_{t\in[T]}\sum_{i\in[K]} p_t \cdot x_{i,t}^* + h(x_{i,t}^*) \leq Z^*(\boldsymbol{s}_1, N_{f,1}; \bar{\boldsymbol{D}}) = \Gamma.$$

Thus, all the constraints in problem (20) are satisfied. Since $\theta_t = 1$ is a feasible solution for all t, we have $\boldsymbol{\theta}^* \leq 1$. $\square$

Appendix B: Incorporating transmission-capacity constraints

The formulation can be extended directly to incorporate station-level transmission-capacity limits of the form

$$\sum_{i\in[K]} \frac{Bx_{i,t}}{L} \leq C_t, \quad \forall t \in [T], \tag{24}$$

where L is the period length, B is the battery capacity, and C_t is the transmission capacity made available by the local grid after accounting for non-battery electricity load. Since B and L are constants, this is equivalent to the linear constraint $\sum_{i\in[K]} x_{i,t} \leq \bar{C}_t$, where $\bar{C}_t := C_t L/B$. Hence the extension can be incorporated into the DP feasible set simply by replacing $\mathcal{X}_t(\boldsymbol{s}_t, N_{f,t})$ with

$$\mathcal{X}_t^{\mathrm{tc}}(\boldsymbol{s}_t, N_{f,t}) := \left\{ (\boldsymbol{x}_t, \boldsymbol{z}_t) \in \mathcal{X}_t(\boldsymbol{s}_t, N_{f,t}) \;\middle|\; \sum_{i\in[K]} x_{i,t} \leq \bar{C}_t \right\}.$$

The same linear constraint can be added period by period to the RS, MPCSAA, and Wasserstein-DRO rolling-horizon formulations without changing the overall algorithmic structure.

To gauge the practical effect of (24), we ran a one-day probe under the baseline numerical setting $N = 40$, $K = 20$, $|S| = 20$, and $\beta = 0.6$, and imposed a stylized time-varying capacity profile with $C_t = 1200$ kW in off-peak hours and $C_t = 1000$ kW during daytime peak hours. In the unconstrained baseline run, the implemented charging power never exceeded 592 kW, so the added transmission-capacity limit is slack along the realized trajectory. Consistent with this observation, the service outcome remains unchanged in the probe. The computed rolling decisions can still differ slightly across runs because the mixed-integer problems are solved to a small optimality gap and may admit multiple near-optimal schedules, but the economic structure is unaffected: when the station is well below its grid limit, the transmission-capacity constraint does not change the service-versus-cost trade-off that drives the policy. If the grid limit becomes binding, however, the operator would need to ration charging power across bays, which would effectively truncate the unconstrained policy by making aggregate charging power, rather than only battery inventory, the scarce operational resource.

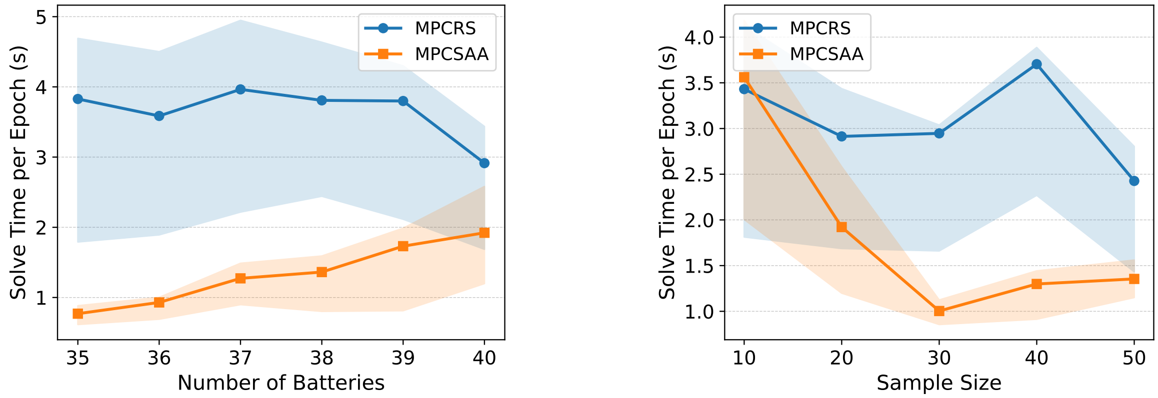

(a) Varying the total number of batteries N (b) Varying the in-sample size $|S|$

Figure 8 Runtime comparison based on per-epoch solve times over a representative 24-period day. Solid lines show mean runtime and shaded bands show the interquartile range across the 24 rolling-horizon epochs.

Appendix C: Runtime comparison

In this appendix, we report a clean runtime experiment for the rolling-horizon implementation of MPCRS and MPCSAA. We use the same solver formulations, parameter values, and random seeds as in the numerical study, but focus on a representative 24-period day and record the solve time of each optimization run at every decision epoch. This produces 24 runtime observations for each method under each parameter setting. To avoid overly concentrated box plots, Figure 8 summarizes these observations by plotting the mean runtime together with the interquartile range, which makes the cross-setting trends easier to read.

Figure 8a varies the total number of batteries N while fixing $|S| = 20$, and Figure 8b varies the in-sample size $|S|$ while fixing $N = 40$. Across these settings, both methods remain computationally practical for hourly re-optimization. In the experiment that varies N, the mean per-epoch runtime of MPCRS is between roughly 2.9 and 4.0 seconds, while the corresponding mean runtime of MPCSAA ranges from about 0.8 to 1.9 seconds. In the experiment that varies $|S|$, the mean per-epoch runtime of MPCRS stays between about 2.4 and 3.7 seconds, whereas MPCSAA ranges from about 1.0 to 3.6 seconds. These results confirm that MPCRS imposes an additional but still moderate solve-time burden relative to MPCSAA.

Appendix D: Sensitivity to the budget parameter β

In this appendix, we examine the sensitivity of MPCRS to the forecast-scaling parameter β used in the budget construction $\hat{\boldsymbol{D}} = \bar{\boldsymbol{D}} + \beta\boldsymbol{\sigma}$. To make the service-side trade-off more visible, we use the tighter inventory setting $N = 35$ with $K = 20$ and $|S| = 20$, and consider $\beta \in \{0.2, 0.4, 0.6, 0.8, 1.0\}$. For each value, we rerun a 10-day seeded simulation under the same rolling-horizon design and solver settings as in the main numerical study. The figure reports service shortfall and the fraction of backlog hours in percentage terms, which makes the remaining differences easier to compare across β.

Figure 9 shows a clearer trade-off than in the more capacitated case. As β increases, the cost budget becomes more conservative and the mean total cost rises from about 345.8 at $\beta = 0.2$ to about 375.9 at $\beta = 1.0$. At the same time,

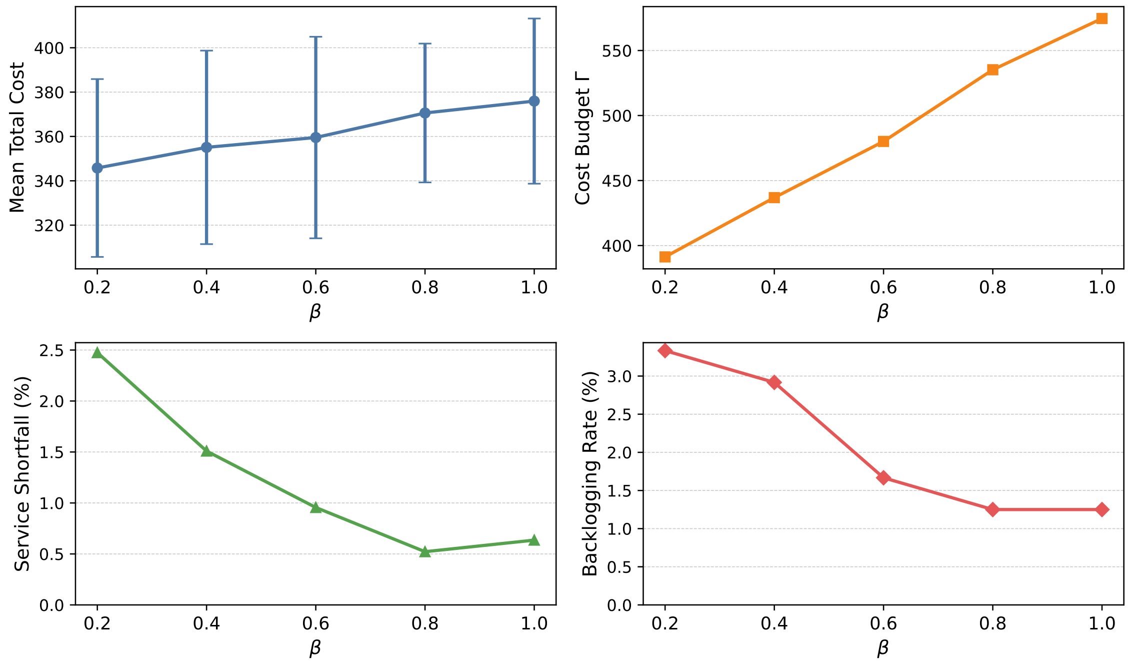

Figure 9 **Sensitivity of MPCRS performance to the budget parameter β under the tighter inventory setting $N = 35$, with $K = 20$, $|S| = 20$, and a 10-day seeded simulation design. The panels report total cost, the implied cost budget, aggregate service shortfall, and the fraction of backlog hours.**

the mean aggregate service shortfall falls from about 2.47% at $\beta = 0.2$ to about 0.96% at $\beta = 0.6$, and then to about 0.52% at $\beta = 0.8$. The fraction of backlog hours also declines, from about 3.33% at $\beta = 0.2$ to about 1.25% at $\beta = 0.8$. However, the reliability improvement is not strictly monotone at the highest β value in this finite simulation: at $\beta = 1.0$, the mean service shortfall increases slightly to about 0.64% while the fraction of backlog hours remains at 1.25%. This evidence still supports the interpretation of β as a conservatism lever, but it also suggests diminishing returns beyond moderate values. In particular, $\beta = 0.6$ provides a meaningful service improvement over $\beta = 0.2$ and $\beta = 0.4$ without the larger cost increase associated with $\beta = 0.8$ and $\beta = 1.0$.

Appendix E: Comparison with DRO

To complement the main comparison with MPCSAA, we also consider a Wasserstein-based robust benchmark. A fully standard multistage DRO reformulation of the original dynamic problem is difficult in our setting because demand enters the inventory recursion and hence the state-dependent loading-capacity constraint, leading to path-dependent mixed-integer constraints without an obvious tractable robust counterpart. To obtain a meaningful ambiguity-aware benchmark, we instead directly robustify the deterministic static approximation model. Specifically, we replace period-by-period empirical demand by upper and lower worst-case mean demand profiles derived from Wasserstein balls around the empirical demand distributions. This benchmark remains aligned with the static SAA formulation used in the main numerical comparison.

For each period $t \in [T]$, let $\hat{\mathbb{P}}_t$ denote the empirical distribution of demand and let $\mathcal{B}_\rho(\hat{\mathbb{P}}_t)$ denote the 1-Wasserstein ball of radius ρ centered at $\hat{\mathbb{P}}_t$. Define the upper and lower worst-case mean demands as

$$\bar{d}^{\mathrm{wc}}_{t,+}(\rho) := \sup_{\mathbb{P}_t \in \mathcal{B}_\rho(\hat{\mathbb{P}}_t)} \mathbb{E}_{\mathbb{P}_t}[\tilde{d}_t], \qquad \bar{d}^{\mathrm{wc}}_{t,-}(\rho) := \inf_{\mathbb{P}_t \in \mathcal{B}_\rho(\hat{\mathbb{P}}_t)} \mathbb{E}_{\mathbb{P}_t}[\tilde{d}_t]. \tag{25}$$

The upper worst-case mean is used to protect against demand surges in the cumulative service requirement, while the lower worst-case mean is used in the cumulative loading-capacity constraint, since lower realized demand implies fewer depleted batteries returning to the station.

The resulting robust benchmark is formulated as

$$\begin{aligned}
\underset{(\boldsymbol{x}_t, \boldsymbol{s}_{t+1}, \boldsymbol{z}_t)_{t\in[T]}}{\text{minimize}} \quad & \sum_{t\in[T]} \sum_{i\in[K]} p_t x_{i,t} + h(x_{i,t}) \\
\text{subject to} \quad & \sum_{\tau=1}^{t} \gamma_\tau \bar{d}^{\mathrm{wc}}_{\tau,+}(\rho) \le N_{f,1} + \sum_{\tau=1}^{t} \sum_{i\in[K]} z_{i,\tau}, \qquad \forall t \in [T], \\
& \sum_{i\in[K]} z_{i,t} \le N - K, \qquad \forall t \in [T], \\
& \sum_{\tau=1}^{t} \sum_{i\in[K]} z_{i,\tau} - \sum_{\tau=1}^{t-1} \gamma_\tau \bar{d}^{\mathrm{wc}}_{\tau,-}(\rho) \le N - K - N_{f,1}, \qquad \forall t \in [T], \\
& \text{SOC dynamics and charging-rate constraints are the same as in the MPCSAA model.}
\end{aligned} \tag{26}$$

This benchmark differs from the RS model in two main respects. First, ambiguity is controlled exogenously through the Wasserstein radius ρ, rather than endogenously through the ambiguity-penalty parameter in the RS model. Second, the benchmark directly robustifies the empirical demand input, whereas the RS model constructs an endogenous robust demand target through the auxiliary variable w_t.

When demand is supported on the interval $[0, \bar{d}]$, the worst-case means in (25) admit the simple bounds

$$\bar{d}^{\mathrm{wc}}_{t,+}(\rho) = \min\{\hat{\mu}_t + \rho, \bar{d}\}, \qquad \bar{d}^{\mathrm{wc}}_{t,-}(\rho) = \max\{\hat{\mu}_t - \rho, 0\}, \tag{27}$$

where $\hat{\mu}_t$ is the empirical mean of period-t demand. We use these expressions in the implementation of the benchmark.

We report the benchmark under the same setting used to study the MPCRS baseline in the main numerical section, namely $N = 35$, $K = 20$, and $|S| = 20$, using the same seeds over a 20-day simulation. Table 3 shows the resulting trade-off. When ρ is small, such as $\rho = 0.25$, the DRO benchmark attains a lower mean total cost of 325.66, but aggregate service falls to 0.961 and the day-level backlogging rate rises to 0.75. Increasing ρ improves service protection but raises cost substantially: for $\rho \in \{0.5, 0.75, 1.0\}$, aggregate service lies between 0.978 and 0.982, while the mean total cost rises to about 382–383. By comparison, the saved MPCRS baseline at the same setting achieves aggregate service 0.995, individual service 0.998, mean total cost 347.21, and day-level backlogging rate 0.10. Thus, the DRO benchmark exhibits the expected conservatism trade-off, but across these tested ρ values it does not dominate MPCRS: small ρ values lower cost at the expense of materially weaker service, whereas larger ρ values improve service only partially and still remain more expensive than MPCRS.

Appendix F: DP formulation for random initial SOC

In this section, we relax the assumption that the SOC of unloaded batteries is fixed, and develop the corresponding DP formulation.

Suppose that the charging bays are always loaded with batteries. Let $L = N - K$ be the maximum possible number of drained batteries waiting for loading. We introduce a new state variable $\boldsymbol{r}_t = (r_{1,t}, \ldots, r_{L,t})$, which represents the

Table 3 Twenty-day Wasserstein-DRO results under $N = 35$, $K = 20$, and $|S| = 20$. The backlogging rate is the fraction of simulated days with non-full individual service.

ρ	Aggregate service	Ind. service	Total cost	Backlogging rate	Mean runtime (s)
0.25	0.961	0.974	325.66	0.75	6.91
0.50	0.980	0.991	383.08	0.45	0.45
0.75	0.978	0.989	381.88	0.60	0.51
1.00	0.982	0.991	383.16	0.55	0.47

SOC of drained batteries. Note that the total number of such batteries is at most L, meaning that only some of the elements of $\boldsymbol{r}$ are positive. All the rest values serve as dummy variables for modeling purposes, and we set these values to zero. Given this state variable, we introduce additional decision variables $\boldsymbol{y}_{i,t} = (y_{i,1,t}, \dots, y_{i,L,t})$ to represent whether load drained battery $j \in [L]$ to charging bay $i \in [K]$ in period t.

In this setting, the battery inventory dynamics do not change, but the SOC dynamics are rewritten as the following equation

$$s_{i,t+1} = s_{i,t}(1 - z_{i,t}) + x_{i,t} + \sum_{j \in [L]} r_{j,t} y_{i,j,t}, \tag{28}$$

where decision $\boldsymbol{y}_{i,t}$ is subject to the following constraints

$$\sum_{j \in [L]} y_{i,j,t} = z_{i,t} \quad \forall i \in [K] \tag{29}$$

and

$$\sum_{i \in [K]} y_{i,j,t} \le 1 \quad \forall j \in [L], \quad \sum_{i \in [K]} y_{i,j,t} \le M \cdot r_{j,t} \quad \forall j \in [L]. \tag{30}$$

where M is a big positive constant.

Constraint (29) says that exactly one of the L drained batteries are loaded to charging bay i if it is available. Constraint (30) says that one drained battery can be loaded onto at most one charging bay, if the corresponding drained battery has nonzero SOC, i.e., battery j is not a dummy variable.

Given the above constraints, the decision space can be written as follows.

$$\mathcal{X}_t(\boldsymbol{s}_t, \boldsymbol{r}_t, N_{f,t}) = \left\{ (\boldsymbol{x}_t, \boldsymbol{Y}_t, \boldsymbol{z}_t) \left| \begin{array}{l} \boldsymbol{x}_t \in [0, \bar{x}]^K, \boldsymbol{z}_t \in \{0,1\}^K, \boldsymbol{y}_t \in \{0,1\}^L \\ \mathbb{E}\left[\min\left\{N_{f,t} + \sum_{i \in [K]} z_{i,t}, \tilde{d}_t\right\}\right] \ge \gamma_t \mathbb{E}\left[\tilde{d}_t\right] \\ s_{i,t}(1 - z_{i,t}) + x_{i,t} + \sum_{j \in [L]} r_{j,t} y_{i,j,t} \le 1 \quad \forall i \in [K] \\ \text{Constraints (2), (3), (29), (30)} \end{array} \right. \right\} \tag{31}$$

where $\boldsymbol{Y}_t := (\boldsymbol{y}_{i,t})_{i \in [K]}$.

The optimal cost-to-go of each period satisfies the following Bellman equation

$$V_t^*(\boldsymbol{s}_t, \boldsymbol{r}_t, N_{f,t}) = \min_{(\boldsymbol{x}_t, \boldsymbol{Y}_t \boldsymbol{z}_t) \in \mathcal{X}_t(\boldsymbol{s}_t, \boldsymbol{r}_t, N_{f,t})} c_t(\boldsymbol{x}_t) + g(\boldsymbol{x}_t) + \mathbb{E}\left[V_{t+1}^*(\boldsymbol{s}_{t+1}, N_{f,t+1})\right], \tag{32}$$

where the expectation is taken with respect to the random SOC and demand, and boundary condition is $V_{T+1} = C \cdot \mathbb{E}\left[(-N_{f,T+1})^+\right]$. The state transition equations are given by (28) and (4).

We see that the above DP is even harder than (9) due to lifted state space and decision space.

In the next section, instead of solving the DP formulation in (32) we numerically examine the impact of random initial SOC on the performance of our method.

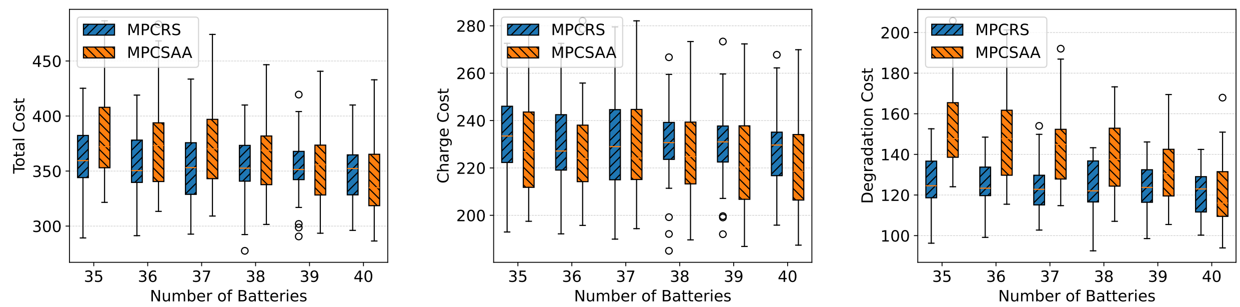

(a) Total Cost (b) Charge Cost (c) Degradation Cost

Figure 10 Comparison of costs across methods as N varies.

Table 4 Comparison of measures across N and methods

N	Method	Agg Service Rate Mean	Agg Service Rate Std	Ind Service Rate Mean	Ind Service Rate Std	Total Cost Mean	Total Cost Std	Backlogging Rate
35	MPCRS	**0.997**	**0.010**	**0.998**	**0.008**	**360.239**	**38.731**	**0.100**
	MPCSAA	0.980	0.037	0.990	0.019	384.169	43.633	0.500
36	MPCRS	**0.996**	**0.016**	0.995	0.020	**356.530**	**36.686**	**0.100**
	MPCSAA	0.989	0.018	0.995	**0.008**	376.969	47.411	0.450
37	MPCRS	**0.995**	0.014	0.997	0.012	**355.554**	**38.748**	**0.200**
	MPCSAA	0.993	0.014	0.997	**0.006**	373.051	46.224	0.250
38	MPCRS	**0.998**	**0.006**	0.997	0.011	**352.820**	**35.241**	**0.100**
	MPCSAA	0.996	0.007	**0.998**	**0.003**	365.651	42.415	0.300
39	MPCRS	**0.999**	**0.004**	0.997	0.011	**353.555**	**34.372**	**0.050**
	MPCSAA	0.997	0.008	**0.999**	**0.002**	356.746	40.860	0.150
40	MPCRS	0.999	**0.004**	0.997	0.011	349.929	**33.153**	0.050
	MPCSAA	0.999	0.006	**0.999**	**0.002**	**344.455**	40.045	0.050

Appendix G: Impact of random SOC.

Based on the stochastic DP formulation in online Appendix F, we can easily extend our framework and the benchmark to the setting with random SOC. However, the resulting MICP can be intractable due to the additional binary decisions in the high dimensional decision space. Thus, to examine the impact of random SOC on the performance comparison, we perform the simulation by uniformly sample SOCs from the interval $[0.05, 0.15]$ for each battery loaded onto the charging bay, and all the rest settings are consistent with the experiment in Section 5.2. We summarize the results in Figure 10 and in Table 4. Similar to the observation in Section 5.2, the battery degradation cost and total cost of our method are consistently lower than MPCSAA, while the service levels of these two methods are close to each other. In addition, our method achieves lower backlogging rate.

Appendix H: Static SAA formulation

In this section, we develop the SAA formulation for the static charging problem, that is, the charging decisions are not adaptive to demand realization. Given demand samples $(\hat{\boldsymbol{d}}_s)_{s\in[S]}$, the formulation is given as follows:

$$
\begin{aligned}
\underset{(\boldsymbol{x}_t,\boldsymbol{s}_{t+1},\boldsymbol{z}_t,\boldsymbol{q}_t)_{t\in[T]}}{\text{minimize}} \quad & \sum_{t\in[T]}\sum_{i\in[K]} p_t\cdot x_{i,t} + h(x_{i,t}) \\
\text{subject to} \quad & \frac{1}{S}\sum_{s\in[S]} \min\left\{N_{f,1} + \sum_{i\in[K]}\sum_{j=1}^{t} z_{i,j} - \sum_{j=1}^{t-1}\hat{d}_{j,s}, \hat{d}_{t,s}\right\} \geq \gamma_t\cdot\frac{1}{S}\sum_{s\in[S]}\hat{d}_{t,s} \;\; \forall t\in[T] \\
& \sum_{i\in[K]} z_{i,t} \leq N-K \qquad \forall t\in[T] \\
& \sum_{i\in[K]}\sum_{j=1}^{t} z_{i,j} - \sum_{j=1}^{t-1}\hat{d}_{j,s} \leq N-K-N_{f,1} \qquad \forall t\in[T]\; \forall s\in[S] \\
& \text{Constraints } (2),(11) \\
& \boldsymbol{x}_t\in[0,x_u]^K, \boldsymbol{z}_t\in\{0,1\}^K, \boldsymbol{s}_{t+1}\in[0,1]^K \qquad \forall t\in[T]
\end{aligned}
\tag{33}
$$

where we define $\sum_{j=1}^{0}\hat{d}_{j,s}=0$ for $s\in[S]$.

In the above model, the first constraint is the service level constraint, and the second and third one are capacity constraints. By introducing auxiliary variables $v_{t,s}$, this model can be further simplified as the following MICP:

$$
\begin{aligned}
\underset{(\boldsymbol{x}_t,\boldsymbol{s}_{t+1},\boldsymbol{z}_t,\boldsymbol{q}_t,\boldsymbol{v}_t)_{t\in[T]}}{\text{minimize}} \quad & \sum_{t\in[T]}\sum_{i\in[K]} p_t\cdot x_{i,t} + h(x_{i,t}) \\
\text{subject to} \quad & \frac{1}{S}\sum_{s\in[S]} v_{t,s} \geq \gamma_t\cdot\frac{1}{S}\sum_{s\in[S]}\hat{d}_{t,s} \qquad \forall t\in[T] \\
& v_{t,s} \leq N_{f,1} + \sum_{i\in[K]}\sum_{j=1}^{t} z_{i,j} - \sum_{j=1}^{t-1}\hat{d}_{j,s} \qquad \forall t\in[T]\; \forall s\in[S] \\
& v_{t,s} \leq \hat{d}_{t,s} \qquad \forall t\in[T]\; \forall s\in[S] \\
& \sum_{i\in[K]} z_{i,t} \leq N-K \qquad \forall t\in[T] \\
& \sum_{i\in[K]}\sum_{j=1}^{t} z_{i,j} - \sum_{j=1}^{t-1}\hat{d}_{j,s} \leq N-K-N_{f,1} \qquad \forall t\in[T]\; \forall s\in[S] \\
& \text{Constraints } (2),(11) \\
& \boldsymbol{x}_t\in[0,x_u]^K, \boldsymbol{z}_t\in\{0,1\}^K, \boldsymbol{s}_{t+1}\in[0,1]^K \qquad \forall t\in[T]
\end{aligned}
\tag{34}
$$

We can introduce slack variables to the service level constraints to ensure feasibility when solving the above MICP.

Appendix I: Comparison with Related Literature

In Table 5, we summarize the main differences between our work and the most related papers.

Appendix J: Estimation of battery degradation cost parameter

Let $g(x_i)$ denote the degradation cost per kWh, and consider the point estimates of battery degradation cost in Table 6.

In this table, we consider 5 charging rates: 0.5, 1, 1.5, 2, 3. Drawn from industry sources and academic studies, we first estimate the empirical cycle-life of batteries under these charging rates. Specifically, Battery University's data

Table 5 Positioning relative to closely related battery-swapping and EV-charging studies.

Reference	Scope	Demand	Charging-rate control	Service protection	Difference from this paper
Tan et al. (2017)	Single station	Deterministic	Continuous decision	Inventory tracked	No stochastic demand, rolling service protection, or threshold result.
Widrick et al. (2018)	Single station	Stochastic	Fixed-rate / not decision	Inventory state in MDP	No continuous charging or degradation trade-off.
Sun et al. (2017)	Single station	Stochastic	Fixed-rate / not decision	Explicit QoS constraint	Queueing MDP with QoS control; no continuous charging-rate optimization.
Schneider et al. (2018)	Station network	Stochastic	Fixed rate / not decision	Network balancing	Network-level transshipment model; no charging rate control.
Qi et al. (2023)	Citywide planning network	Deterministic planning	No charging-rate decision	Repairable-inventory design	Planning model for network design; no charging-rate decision.
This paper	Single station	Stochastic, ambiguous	Fixed, two-rate, and continuous decision	Explicit service-level protection	Charging rate control with service protection, degradation, and the operational value of charging-rate flexibility.

Table 6 Point Estimate of Degradation Cost

x (C-rate)	$L(x)$ (cycles)	$g(x_i)$ ($/kWh)
0.5	2000	0.040
1	1200	0.067
1.5	800	0.100
2	450	0.178
3	300	0.267

shows at 2C discharge, cycle life to half-capacity is roughly 450 cycles [2]. EVreporter reports that modern NMC 18650 cells achieve about 1200 cycles at 1C before 20% degradation [3]. An accelerated aging study on $LiFePO_4$/graphite cells lists cycle lives near 800 cycles under a 1.5C protocol [4]. CALCE's open-access test data confirms that lower C-rates (0.5C) can exceed 2000 cycles before reaching end-of-life criteria [5]. Finally, Nature Energy notes that at 3C protocols, many cells still deliver 300–400 cycles in lab tests [6].

[2] BU-501a: Discharge Characteristics of Li-ion; Retrieved from https://batteryuniversity.com/article/bu-501a-discharge-characteristics-of-li-ion

[3] Understanding Charge-Discharge Curves of Li-ion Cells; Retrieved from https://evreporter.com/understanding-charge-discharge-curves-of-li-ion-cells/

[4] Sun, S., Guan, T., Zuo, P., Gao, Y., Cheng, X., Du, C., & Yin, G. (2018). Accelerated aging analysis on cycle life of LiFePO4/graphite batteries based on different rates. ChemElectroChem, 5(16), 2301-2309.

[5] Battery Data; Retrieved from https://calce.umd.edu/battery-data

[6] Geslin, A., Xu, L., Ganapathi, D., Moy, K., Chueh, W. C., & Onori, S. (2025). Dynamic cycling enhances battery lifetime. Nature Energy, 10(2), 172-180.

The cost of EV battery has declined significantly due to the rapid growth of EV market. According to a report by Goldman Sachs, we estimate the cost of battery pack as $C_{\text{pack}} = 80$\$/kWh [7]. We then calculate the corresponding $g(x_i)$ based on the following formula

$$g(x_i) \approx \frac{C_{\text{pack}}}{L(x_i)}.$$

Based on the above results, we then solve the following least square problem to estimate parameter b

$$\min_b \sum_{i=1}^{5} \left(ax_i^2 - g(x_i)\right),$$

of which the closed-form solution is

$$b = \frac{\sum_{i=1}^{5} x_i^2 g(x_i)}{\sum_{i=1}^{5} x_i^4} \approx 0.058 \text{ \$kWh}.$$

[7] Electric vehicle battery prices are expected to fall almost 50% by 2026; Retrieved from https://www.goldmansachs.com/insights/articles/electric-vehicle-battery-prices-are-expected-to-fall-almost-50-percent-by-2025